PHYSICS AND CHEMISTRY OF SOLID STATE
V. 26, No.4 (2025) pp. 787-793

Section: Chemistry

DOI: 10.15330/pcss.26.4.787-793

Vasyl Stefanyk Carpathian National University

ФІЗИКА І ХІМІЯ ТВЕРДОГО ТІЛА
Т. 26, № 4 (2025) С. 787-793

Хімічні науки

UDK: 537.311.322

ISSN 1729-4428 (Print)
ISSN 2309-8589 (Online)

L. Romaka[1], Yu. Stadnyk[1], V.A. Romaka[2], A. Horyn[1], V.V. Romaka[3,4], P. Demchenko[1], P. Haranyuk[2]

Research on a new thermoelectric material obtained by doping of *n*-HfNiSn with Nb atoms

[1]*Ivan Franko National University of Lviv, Lviv, Ukraine,* lyubov.romaka@gmail.com;
[2]*National University "Lvivska Politechnika", Lviv, Ukraine,* volodymyr.romaka@gmail.com;
[3]*Technische Universität Dresden, Chair of Inorganic Chemistry II, Dresden, Germany,*
vitaliy.romaka@tu-dresden.de
[4]*Institute for Solid State Research, IFW-Dresden, Dresden, Germany*

The structural, kinetic, energetic, and magnetic properties of the new thermoelectric material $Hf_{1-x}Nb_xNiSn$, obtained by doping the *n*-HfNiSn semiconductor with Nb atoms introduced into the structure by substituting Hf atoms in the crystallographic position 4*a*, have been investigated. It has been established that at concentrations of x=0.02 inclusive, there is a solid solution of $Hf_{1-x}Nb_xNiSn$ substitution of Hf atoms ($5d^26s^2$) for Nb atoms ($4d^45s^1$). In this case, defects of donor nature are generated in the $Hf_{1-x}Nb_xNiSn$ structure (Nb contains more *d*-electrons than the Hf atom), and impurity donor states ε_D appear in the band gap ε_g. At concentrations of $0.02<x\leq0.05$, substitution probably occurs by displacing Ni atoms from position 4*a*, which in the original HfNiSn compound was occupied by a statistical mixture of Hf and Ni atoms. In this case, defects of an acceptor nature are generated in the $Hf_{1-x}Nb_xNiSn$ structure (Nb contains fewer *d*-electrons than the Ni atom), and impurity acceptor states ε_A appear in the band gap ε_g. The ratio of donor and acceptor states determines the type of conductivity of $Hf_{1-x}Nb_xNiSn$. It is shown that the semiconductive solid solution $Hf_{1-x}Nb_xNiSn$ is highly efficient in converting thermal energy into electrical energy.

Keywords: semiconductor, electrical conductivity, thermopower coefficient, Fermi level.

Received 24 November 2024; Accepted 12 November 2025.

Introduction

Thermoelectric materials based on half-Heusler semiconductor phases MNiSn (M – Ti, Zr, Hf) (MgAgAs structure type, space group $F\bar{4}3m$ [1]) have high efficiency of converting thermal energy into electrical energy [2]. To achieve maximum values of thermoelectric figure of merit Z ($Z=\alpha^2\cdot\sigma/\kappa$), doping of basic MNiSn semiconductors with donor and/or acceptor impurities is carried out, which allows to purposefully change the values of electrical conductivity σ, thermopower coefficients α and thermal conductivity κ [3, 4].

The authors of Ref. [5] studied the structural, kinetic, energy, and magnetic properties of the *n*-HfNiSn semiconductor and established regularities in the change of its fundamental parameters. *X*-ray structural studies of alloys in the $HfNi_{1+x}Sn$ region revealed the existence of a homogeneity range for the HfNiSn compound. Clarification of the occupancy of positions in HfNiSn showed the presence of a statistical mixture of Hf and Ni atoms in the Hf (4*a*) position. In turn, the replacement of Hf atoms ($5d^26s^2$) by Ni atoms ($3d^84s^2$) leads to the appearance of defects of donor nature in the HfNiSn structure (Ni has more *d*-electrons) and impurity donor states ε_D in the band gap ε_g, which will force the Fermi level ε_F to drift to the conduction band ε_C. In this case, the width of the band gap ε_g of the semiconductor also changes.

Modeling of the electronic structure by the KKR-CPA-LDA method [6] and electrokinetic studies of the half-Heusler HfNiSn phase confirmed the conclusions of structural studies. Calculation of DOS assuming an ordered variant of the structure of the HfNiSn compound shows that it is an *n*-type semiconductor, and the Fermi level ε_F is located in the conduction band ε_C. However, this variant of the DOS calculation does not agree with the results of kinetic studies, which show the location of the Fermi level ε_F in the band gap ε_g.

The DOS calculation for the disordered variant of the structure $(Hf_{1-x}Ni_x)NiSn$ allowed us to choose a model of the structure as close as possible to the real one based on the nature of the change in the density of electronic states at the Fermi level $g(\varepsilon_F)$. Such a characteristic point is the minimum in the $g(\varepsilon_F)(x)$ dependence, which exists for the disordered model described by the formula $(Hf_{0,99}Ni_{0,01})NiSn$. The resulting semiconductor has a band gap ε_g=282 meV, and the Fermi level ε_F is located in the band gap ε_g near the conduction band ε_C, which indicates an electronic type of conduction and implies the activation of electrons from the Fermi level ε_F into the conduction band ε_C.

A feature of doping of *n*-HfNiSn with rare-earth metal atoms, as well as *d*- and *p*-metals, is the ordering of the crystal structure of the semiconductor, which redistributes the density of electronic states at the Fermi level $g(\varepsilon_F)$ [2]. If structural defects of donor nature exist in HfNiSn as a result of displacement of up to ~1% of Hf atoms by Ni atoms, then ordering of the structure, for example, in $Hf_{1-x}Y_xNiSn$ leads to a decrease in the number of donors, since Ni atoms leave the position of Hf atoms (4*a*) ("healing" of defects of donor nature) [7]. In this context, it is interesting to study the intermetallic semiconductor *n*-HfNiSn, heavily doped with Nb impurity ($4d^45s^1$), introduced into the structure by substituting Hf atoms ($5d^26s^2$) in the crystallographic position 4*a*. Since the Nb atom contains more *d*-electrons than the Hf atom, we expected the appearance of structural defects of donor nature and impurity donor states ε_D in the band gap ε_g. By changing the concentration of such states, we can change the compensation degree of the $Hf_{1-x}Nb_xNiSn$ semiconductor and the mechanisms of electrical conductivity. This allows us to optimize the kinetic properties of the thermoelectric material to increase the efficiency of converting thermal energy into electrical energy [2, 3].

The results of the study of the structural, kinetic, energy, and magnetic properties of the intermetallic semiconductor *n*-HfNiSn doped with an Nb impurity, as well as their comparison with the results of electronic structure modeling, will allow us to identify the mechanisms of electrical conductivity to determine the conditions for the synthesis of thermoelectric materials with the maximum efficiency of converting thermal energy into electrical energy, are presented below.

I. Research methods

Samples $Hf_{1-x}Nb_xNiSn$, x= 0.01–0.10, were produced by the arc-melting of the charge of the starting components (the content of the main component is not lower than 99.9 wt. %) in an atmosphere of purified argon (sponge titanium was used as a getter). To give the alloys an equilibrium state, homogenizing annealing was performed at 1073 K for 700 h with subsequent quenching in cold water without breaking the ampoules. *X*-ray phase and *X*-ray structural analyses were performed using diffraction data obtained on DRON-2.0 m (Fe K_α radiation) and STOE STADI P (Cu $K_{\alpha1}$ radiation) diffractometers. The chemical composition of the samples was controlled by the energy-dispersive *X*-ray spectroscopy (Tescan Vega 3 LMU electron microscope). The structural parameters of the $Hf_{1-x}Nb_xNiSn$ solid solution samples were calculated using the Fullprof Suite program [8]. For the ordered variant of the $Hf_{1-x}Nb_xNiSn$ crystal structure, the electronic structure was simulated by the KKR method (Corringa-Kohn-Rostocker method) in the coherent potential CPA and the local density LDA approximations [6]. For the KKR calculations, the licensed AkaiKKR and SPR-KKR software in the LDA approximation for the exchange-correlation potential with the Moruzzi-Janak-Williams (MJW) parameterization [9] were used. The Brillouin zone was divided into 1000 *k*-points, which were used to simulate the energy wave properties by calculating the DOS. The energy window width was 22 eV and was chosen to capture all semi-core states of *p*-elements. The accuracy of calculating the Fermi level position ε_F is ±4 meV. To investigate the electrical transport properties, the samples of regular geometric shapes were manufactured using electric spark-cutting techniques. The temperature dependences of the electrical resistivity $\rho(T)$ were measured by the two-probe method, the thermopower coefficients $\alpha(T)$ relative to copper in the temperature range 80–400 K. The voltage drop was measured in different current directions to reduce the influence of "parasitic" effects at the contact areas. The specific magnetic susceptibility of the $Hf_{1-x}Nb_xNiSn$ samples $\chi(x)$ was measured by the Faraday method at room temperature.

II. Study of the structural properties of $Hf_{1-x}Nb_xNiSn$

X-ray phase and structural analyses, as well as energy-dispersive *X*-ray spectroscopy of $Hf_{1-x}Nb_xNiSn$ samples, showed that they crystallize in the MgAgAs structure type [1] and the X-ray diffraction patterns do not show reflections of other phases. Fig. 1, as an example, shows a microphotograph of the surface and a diffraction pattern of the $Hf_{0.98}Nb_{0.02}NiSn$ sample.

The unit cell parameter $a(x)$ of the $Hf_{1-x}Nb_xNiSn$ samples, calculated from the diffraction data, x = 0–0.10, revealed a complex behavior with a change in the concentration of Nb atoms (Fig. 2, curve 2). At Nb concentrations x = 0–0.02, the value of the unit cell parameter $a(x)$ of $Hf_{1-x}Nb_xNiSn$ predictably decreases since the atomic radius of Nb (r_{Nb}=0.146 nm) is smaller than the atomic radius of Hf (r_{Hf}=0.158 nm). Since the Nb atom ($4d^45s^1$) contains more *d*-electrons than the Hf atom ($5d^26s^2$), in a semiconductor of the electronic conduction type, structural defects of a donor nature will be generated in the range of impurity atom concentrations $0 < x \leq 0.02$, and in the band gap ε_g, the concentration of donor states ε_D will increase, which in the experiment should cause a rapid decrease in the resistivity values.

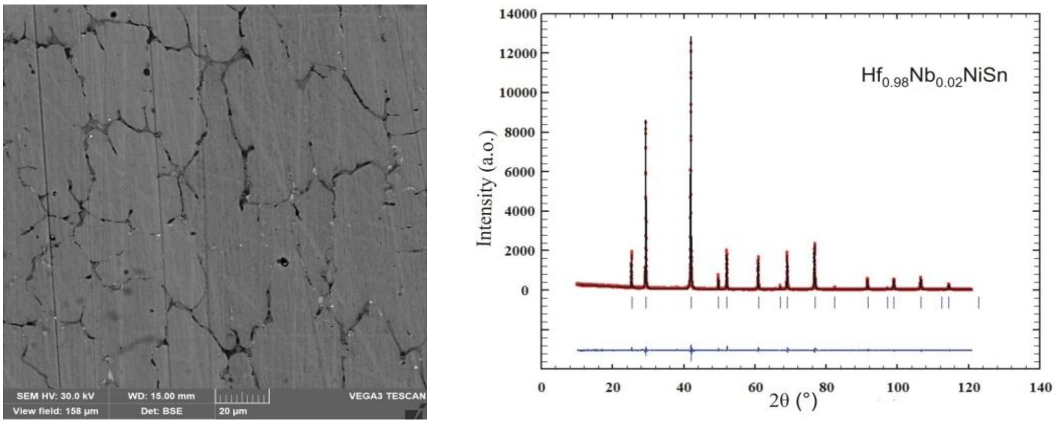

a b

Fig. 1. Microphotograph (a) and X-ray powder pattern (b) of the $Hf_{0.98}Nb_{0.02}NiSn$ sample.

The results of the calculation by the KKR method (AkaiKKR program package [6]) of changes in the values of the unit cell parameter $a(x)$ of $Hf_{1-x}Nb_xNiSn$, $x = 0–0.10$, assuming that Hf atoms are substituted by Nb atoms in the crystallographic position 4*a*, show a linear decrease in the unit cell parameter (Fig. 2, curve 1). Such a decrease in the $a(x)$ values is predictable since the atomic radius of Nb is smaller than that of Hf. At the same time, as can be seen from Fig. 2, in the concentration range $x = 0–0.02$, the rate of decrease in unit cell parameter of the the $Hf_{1-x}Nb_xNiSn$ is practically the same for both the case of simulation and experiment (the angles of inclination of the dependencies $a(x)$ are close).

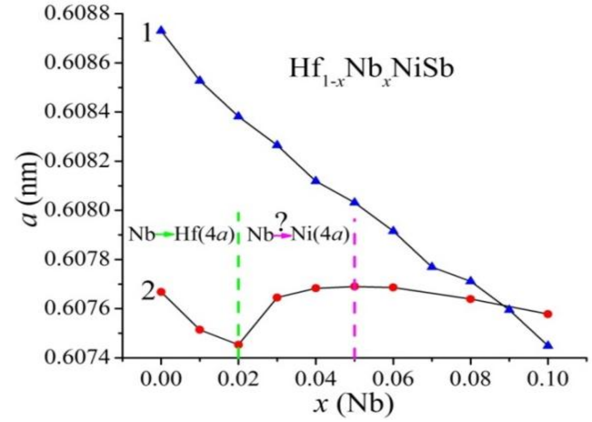

Fig. 2. Variation of the unit cell parameter $a(x)$ of $Hf_{1-x}Nb_xNiSn$:1 – simulation; 2 – experiment.

In this context, we draw attention to the significant difference in the values of the unit cell parameter *a* of the HfNiSn compound obtained from *X*-ray structural studies and modeling data (Fig. 2). The unit cell parameter *a* of the HfNiSn compound calculated from the diffraction data is a_{exp}=0.60767 nm. The one obtained by modeling is larger and equal to a_{mod}=0.608731 nm. Such a significant difference is evidence of the existence of a homogeneity range for the HfNiSn compound and the disorder of its crystal structure due to the substitution of up to ~1% of Hf atoms by Ni atoms [5]. Since the atomic radius of Ni (r_{Ni}=0.125 nm) is much smaller than the atomic radius of Hf (r_{Hf}=0.158 nm), the substitution of up to ~1% of Hf atoms from the crystallographic position 4*a* by Ni atoms will lead to a decrease in the integral value of the unit cell parameter of the HfNiSn compound. This is the reason for the difference in the values of the unit cell parameter of the HfNiSn compound obtained from the experiment and simulation data.

At higher concentrations of Nb impurity ($x > 0.02$), the values of the unit cell parameter $a(x)$ of $Hf_{1-x}Nb_xNiSn$ samples rapidly increase, and this growth in the concentration range $x = 0.02–0.05$ occurs at different rates (different slope of the dependence $a(x)$). At even higher concentrations of Nb atoms, $x > 0.05$, the samples, in addition to the main cubic phase, contain insignificant inclusions of the impurity phase. Therefore, the study of the electrokinetic and magnetic properties of $Hf_{1-x}Nb_xNiSn$ was carried out only for samples with a concentration of Nb atoms $x = 0–0.05$.

To establish the nature of such unexpected behavior of the experimentally determined values of the unit cell parameter $a(x)$ of $Hf_{1-x}Nb_xNiSn$, $x = 0–0.10$, the chemical composition of the samples was determined by *X*-ray spectral analysis (Fig. 3). The presented results of the chemical composition of the $Hf_{1-x}Nb_xNiSn$ samples allow us to assume that the increase in the unit cell parameter $a(x)$ at concentrations of $0.02 < x \leq 0.05$ may be associated with the substitution of Ni atoms (($3d^84s^2$) from position 4*a*, which in the HfNiSn compound they occupied up to ~1% of the positions of Hf atoms [5]. Therefore, at concentrations of $Hf_{1-x}Nb_xNiSn$, $0.02 < x \leq 0.05$, a substitutional solid solution may also exist, but now the Nb atoms displace Ni atoms from position 4*a*, which return to their crystallographic position 4*c*. Such structural changes in $Hf_{1-x}Nb_xNiSn$ should lead to the ordering of the crystal structure of the semiconductor. On the other hand, if the ordering of the crystal structure of $Hf_{1-x}Nb_xNiSn$ occurs and Ni atoms (r_{Ni}=0.125 nm) from position 4*a* return to their crystallographic position 4*c*, then their places in position 4*a* (virtual vacancies) are occupied by Nb atoms (r_{Nb}=0.146 nm), which have a larger atomic radius. This is what causes, in our opinion, an increase in the values of the unit cell parameter $a(x)$ of $Hf_{1-x}Nb_xNiSn$ at concentrations $x = 0.02–0.05$. At even higher concentrations of Nb atoms, x>0.05, a decrease in the values of $a(x)$ of $Hf_{1-x}Nb_xNiSn$ is observed (Fig. 2, curve 2).

Considering that the Nb atom ($4d^45s^1$) has fewer *d*-electrons than the Ni atom ($3d^84s^2$), the substitution of Ni atoms by Nb atoms at position 4*a* generates structural

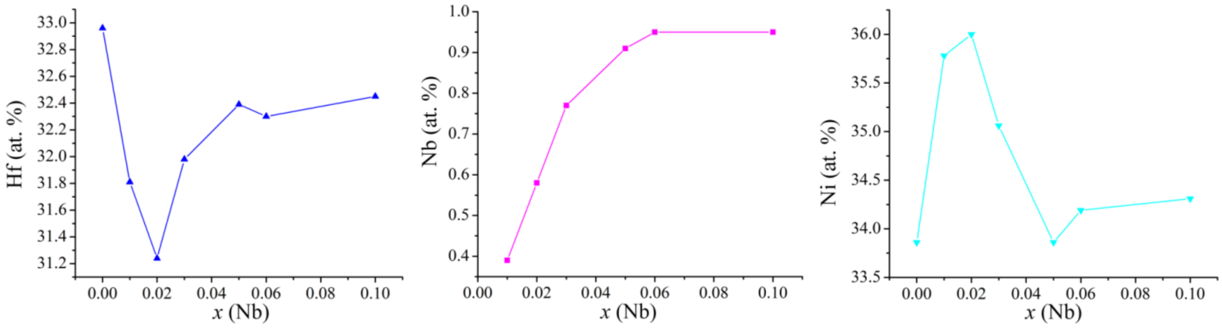

a b c

Fig. 3. Change in the concentration of Hf (a), Nb (b) and Ni (c) atoms in $Hf_{1-x}Nb_xNiSn$ samples according to EPMA data.

defects of acceptor nature in the semiconductor and the corresponding acceptor states ε_A in its band gap ε_g. The generation of acceptor states in the $Hf_{1-x}Nb_xNiSn$ semiconductor of *n*-type conductivity at concentrations $x = 0.02–0.05$ will lead to an increase in the compensation degree and a decrease in the concentration of free electrons due to their capture by acceptors. In this case, the reduction in the resistivity values will slow down in the experiment.

Thus, the results of *X*-ray structural and *X*-ray spectral studies of the *n*-HfNiSn semiconductor doped with Nb atoms showed that in the concentration range $Hf_{1-x}Nb_xNiSn$, $0 < x \leq 0.02$, Nb atoms largely displace Hf atoms from position 4a, generating impurity donor states in the band gap ε_g of the semiconductor, and in the concentration range $x = 0.02–0.05$ they displace Ni atoms from the same position 4*a*, which is accompanied by ordering of the crystal structure and generation of impurity acceptor states. The ratio of donor and acceptor states will determine the type of electrical conductivity (semiconductor or metallic), as well as the main current carriers.

III. Modeling the properties of $Hf_{1-x}Nb_xNiSn$

Calculation of the density of electronic states distribution (DOS) for the ordered variant of the $Hf_{1-x}Nb_xNiSn$ crystal structure allows us to establish the dynamics of changes in the location of the Fermi level ε_F, the band gap width ε_g, and the kinetic properties of the semiconductor (Fig. 4).

As seen from Fig. 4, in *n*-HfNiSn the Fermi level ε_F (dashed line) is located in the band gap ε_g near the edge of the conduction band ε_C, and electrons are the main current carriers. Since the substitution of Hf atoms by Nb atoms generates structural defects of donor nature, then at the impurity concentration $x = 0.005$ in the semiconductor $Hf_{0.995}Nb_{0.005}NiSn$ the Fermi level ε_F will cross the edge of the conduction band ε_C: an insulator-metal transition of conductivity will occur, which is the Anderson transition [10]. In the experiment, we should observe the metallization of the electrical conductivity of $Hf_{1-x}Nb_xNiSn$: activation parts will disappear on the temperature dependences of the resistivity $\ln(\rho(1/T))$, and the electrical resistivity values will increase with temperature due to the action of scattering mechanisms. In this case, the band gap ε_g is preserved in $Hf_{1-x}Nb_xNiSn$.

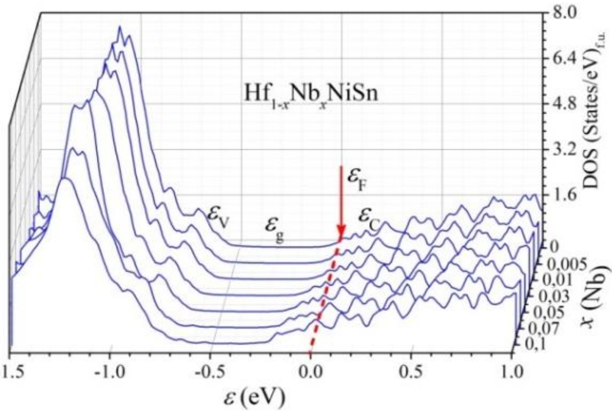

Fig. 4. Modeling of the distribution of the density of electronic states DOS for an ordered variant of the semiconductor structure $Hf_{1-x}Nb_xNiSn$.

IV. Investigation of kinetic and magnetic properties of $Hf_{1-x}Nb_xNiSn$

The study of the behavior of the resistivity ρ (Fig. 5) and the thermopower coefficients α (Fig. 6) of $Hf_{1-x}Nb_xNiSn$ samples showed complete consistency with the conclusions drawn both on the basis of structural studies of the semiconductor and modeling of its electronic structure. As can be seen from Fig. 5*a*, the resistivity values enlarge almost linearly with increasing temperature for each composition of $Hf_{1-x}Nb_xNiSn$.

This nature of the change in the values of $\rho(T,x)$ indicates that even at the lowest concentrations of the Nb impurity in the experiment, which corresponds to the composition of the solid solution $Hf_{1-x}Nb_xNiSn$, $x = 0.01$, the Fermi level ε_F crossed the edge of the conduction band ε_C – an insulator-metal transition of conductivity occurred, and free electrons fully determine the electrical conductivity of the semiconductor. The results of the change in the values of the electrical resistivity $\rho(x,T)$ of $Hf_{1-x}Nb_xNiSn$ at different temperatures (Fig. 5*b*) show that several characteristic regions can be distinguished in the dependences $\rho(x,T)$: $0.01 \leq x \leq 0.03$ and $0.03 \leq x \leq 0.05$. In the first region of Nb impurity concentrations, there is a rapid decrease in the resistivity values $\rho(x,T)$, associated with an increase in the concentration of free electrons when the Fermi level ε_F crosses the conduction band edge ε_C, when Nb atoms largely displace Hf atoms from position 4*a*, generating impurity donor states in the band

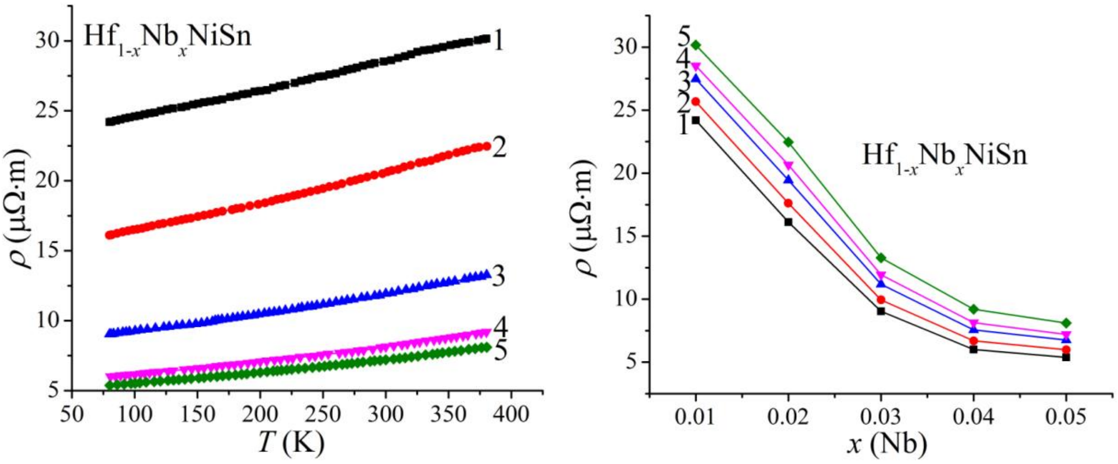

a b

Fig. 5. Temperature (a) and concentration (b) dependences of the resistivity ρ of Hf$_{1-x}$Nb$_x$NiSn;
a: 1 – x=0.01; 2 – x=0.02; 3 – x=0.03; 4 – x=0.04; 5 – x=0.05;
b: 1 – T=80 K; 2 – T=160 K; 3 – T=250 K; 4 – T=300 K; 5 – T=380 K

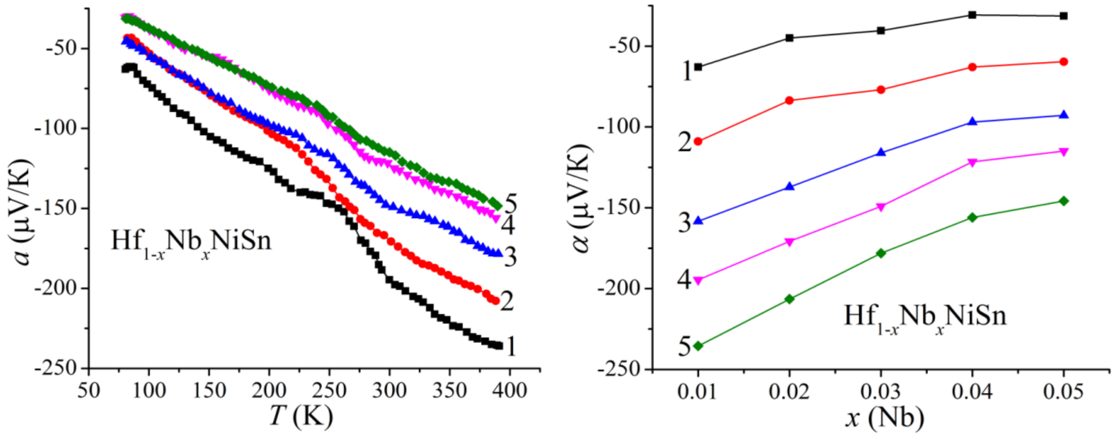

a b

Fig. 6. Temperature (a) and concentration (b) dependences of thermopower coefficients α Hf$_{1-x}$Nb$_x$NiSn;
a: 1 – x=0.01; 2 – x=0.02; 3 – x=0.03; 4 – x=0.04; 5 – x=0.05;
b: 1 – T=80 K; 2 – T=160 K; 3 – T=250 K; 4 – T=300 K; 5 – T=380 K

gap ε_g of the semiconductor.

In the second region, when the Fermi level ε_F is already in the conduction band ε_C, the relative change in the resistivity values $\rho(x,T)$ of Hf$_{1-x}$Nb$_x$NiSn is much smaller than in the first region. We believe that at these concentrations, the impurity Nb atoms now displace Ni atoms to a greater extent from position 4*a*, which is accompanied by the generation of acceptor states that capture free electrons, reducing their concentration. Since at all concentrations of Nb atoms the sign of the thermopower coefficients α of Hf$_{1-x}$Nb$_x$NiSn is negative (Fig. 6), the generated acceptor states are not enough not only to change the type of conductivity of the semiconductor but also to exit the Fermi level ε_F from the conduction band ε_C back to the band gap ε_g, where it was in *n*-HfNiSn.

On the dependences $\alpha(x,T)$ we can also distinguish two similar concentration regions, as on the dependences $\rho(x,T)$, associated with the entry of the Fermi level ε_F into the conduction band ε_C and the generation at concentrations of $0.03 \leq x \leq 0.05$ of impurity acceptor states in the band gap ε_g of the semiconductor Hf$_{1-x}$Nb$_x$NiSn.

The presented results of changes in the values of structural (Fig. 2), energy (Fig. 4) and kinetic properties (Fig. 5, 6) are consistent with the results of experimental measurements of the magnetic susceptibility $\chi(x)$ of Hf$_{1-x}$Nb$_x$NiSn (Fig. 7*a*). Performed studies have shown that the *n*-HfNiSn semiconductor is a weak diamagnet, as evidenced by the negative values of the specific magnetic susceptibility at room temperature. The doping of *n*-HfNiSn with Nb atoms makes the Hf$_{1-x}$Nb$_x$NiSn semiconductor a Pauli paramagnet, in which the magnetic susceptibility is determined exclusively by the electron gas. It is proportional to the density of electronic states at the Fermi level $g(\varepsilon_F)(x)$. As can be seen from Fig. 7*a*, the dependence $\chi(x)$ increases rapidly in the concentration range x = 0–0.02, which we associate with the generation of donor states and an increase in the concentration of free electrons when substituting Hf atoms with Nb atoms. At higher Nb concentrations, the rate of change of the magnetic susceptibility $\chi(x)$ of Hf$_{1-x}$Nb$_x$NiSn, as well as $\rho(x,T)$ and $\alpha(x,T)$, decreases, indicating the generation of acceptor states that capture free electrons, reducing their concentration.

The presented experimental results do not allow us to obtain numerical values of the generation rates of acceptor

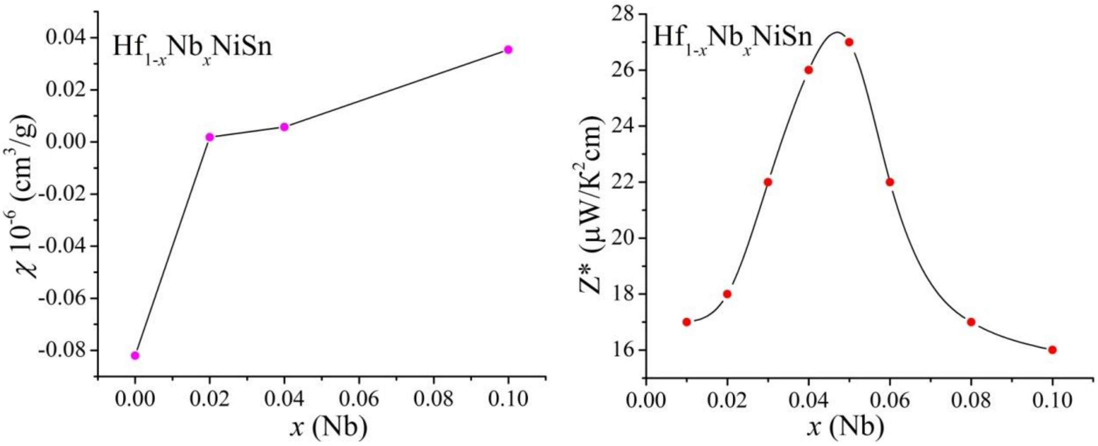

a b

Fig. 7. Change in the values of the specific magnetic susceptibility $\chi(x)$ (a) and the thermoelectric power coefficient $Z^*(x)$ (b) of $Hf_{1-x}Nb_xNiSn$ at T=300 K.

and donor states. This can only be accomplished by comparing the results of experimental measurements of structural and kinetic properties with modeling these properties for different variants of atom distribution in the unit cell. However, these results are beyond the scope of this work.

In the semiconductive solid solution $Hf_{1-x}Nb_xNiSn$, the criterion of achieving maximum values of the thermoelectric power factor Z^* ($Z^*=\alpha^2/\rho$, where α is the thermopower coefficients, ρ is the resistivity) is realized [3]. Fig. 7*b* shows the dependence $Z^*(x)$, from which we can see that the values of the thermoelectric power factor in the semiconductive solid solution $Hf_{1-x}Nb_xNiSn$ are higher than in the undoped semiconductor *n*-HfNiSn. It follows from Fig. 7*b* that at the intersection of the Fermi levels ε_F and the conduction band ε_C when the values of the thermopower coefficients α are still high and the values of the resistivity ρ $Hf_{1-x}Nb_xNiSn$ have rapidly decreased, an extremum occurs on the dependences $Z^*(x)$. It is observed at all studied temperatures. Based on the above results, we can state that the obtained and studied semiconductive solid solution $Hf_{1-x}Nb_xNiSn$ is a promising thermoelectric material.

Conclusions

According to the results of a comprehensive study of the structural, kinetic, energy, and magnetic properties of the new thermoelectric material $Hf_{1-x}Nb_xNiSn$, obtained by doping of the *n*-HfNiSn semiconductor with Nb atoms introduced into the structure by substituting Hf atoms in the crystallographic position 4*a*, it was found that at concentrations x = 0.02 inclusive, there is a solid solution of substitution of Hf atoms ($5d^26s^2$) for Nb atoms ($4d^45s^1$). In this case, defects of a donor nature are generated in the $Hf_{1-x}Nb_xNiSn$ structure (Nb contains more *d*-electrons than the Hf atom), and impurity donor states ε_D appear in the band gap ε_g. It is assumed that at concentrations of $0.02 < x \le 0.05$, there is also a substitutional solid solution, but now Nb atoms displace Ni atoms ($3d^84s^2$) from position 4a, which were in position 4*a* of the HfNiSn compound when substituting up to ~1% of Hf atoms. Thus, in the $Hf_{1-x}Nb_xNiSn$ structure, defects of an acceptor nature are generated (Nb contains fewer *d*-electrons than the Ni atom), and impurity acceptor states ε_A appear in the band gap ε_g. The ratio of donor and acceptor states determines the type of conductivity of $Hf_{1-x}Nb_xNiSn$. It is displayed that the semiconductive solid solution $Hf_{1-x}Nb_xNiSn$ is highly efficient in converting thermal energy into electrical energy.

Acknowledgements

The work was carried out within the framework of grants from the Ministry of Education and Science of Ukraine (No. 0124U000989 and 0124U001146). The authors, L. Romaka, Yu. Stadnyk, A. Horyn, and P. Demchenko, are grateful for the financial support of the Simons Foundation (SFI-PD-Ukraine 00014574).

Romaka Lyubov – Ph.D., Senior Scientist of Ivan Franko National University of Lviv;
Stadnyk Yuriy – Ph.D., Senior Scientist of Ivan Franko National University of Lviv;
Romaka Volodymyr – Proffesor of National University “Lvivska Politechnika”;
Horyn Andriy **–** Ph.D., Senior Scientist of Ivan Franko National University of Lviv;
Romaka Vitaliy – D.Sc., doctor of material science, Technische Universität Dresden, Germany, .
Demchenko Pavlo – Ph.D., Senior Scientist of Ivan Franko National University of Lviv;
Haraniuk Petro **–** docent of National University “Lvivska Politechnika”.

[1] R. Marazza, R. Ferro, G. Rambaldi, *Some phases in ternary alloys of titanium, zirconium, and hafnium, with a MgAgAs or $AlCu_2Mn$ type structure*, J. Less-Common Met. 39, 341 (1975); https://doi.org/10.1016/0022-5088(75)90207-6.

[2] V.A. Romaka, Yu.V. Stadnyk, V.Ya. Krayovskyy, L.P. Romaka, O.P. Guk, V.V. Romaka, M.M. Mykyychuk, A.M. Horyn, *The latest heat-sensitive materials and temperature transducers*, Lviv Polytechnic Publishing House, Lviv (2020); https://opac.lpnu.ua/bib/1131184.

[3] V.A. Romaka, D. Fruchart, Yu.V. Stadnyk, J. Tobola, Yu.K. Gorelenko, M.G. Shelyapina, L.P. Romaka, V.F. Chekurin, *Conditions for attaining the maximum values of thermoelectric power in intermetallic semiconductors of the MgAgAs structural type*, Semiconductors 40(11), 1275, (2006); https://doi.org/10.1134/S1063782606110054.

[4] V.A. Romaka, P. Rogl, Yu.V. Stadnyk, E.K. Hlil, V.V. Romaka, A.M. Goryn, *Features of conductivity of the intermetallic semiconductor n-ZrNiSn heavily doped with a Bi donor impurity*, Semiconductors, 46(7), 887 (2012); https://doi.org/10.1134/S1063782612070172

[5] V.V. Romaka, P. Rogl, L. Romaka, Yu. Stadnyk, A. Grytsiv, O. Lakh, V. Krayovskii, *Peculiarities of structural disorder in Zr- and Hf-containing Heusler and half-Heusler stannides,* Intermetallics 35, 45 (2013); http://dx.doi.org/10.1016/j.intermet.2012.11.022.

[6] M. Schruter, H. Ebert, H. Akai, P. Entel, E. Hoffmann, G.G. Reddy, *First-principles investigations of atomic disorder effects on magnetic and structural instabilities in transition-metal alloys*, Phys. Rev. B 52, 188 (1995); https://doi.org/10.1103/PhysRevB.52.188.

[7] V.A. Romaka, P. Rogl, V.V. Romaka, D. Kaczorowski, V.Ya. Krayovskyy, Yu.V. Stadnyk, and A. M. Horyn, *Features of the Band Structure and Conduction Mechanisms of n-HfNiSn Heavily Doped with Y*, Semiconductors 51(2), 139, (2017). https://doi.org/10.1134/S106378261702018X.

[8] T. Roisnel, J. Rodriguez-Carvajal, *WinPLOTR: a windows tool for powder diffraction patterns analysis*, Mater. Sci. Forum, Proc. EPDIC7 378, 118 (2001); https://doi.org/10.4028/www.scientific.net/MSF.378-381.118.

[9] V. Moruzzi, J. Janak, A. Williams, *Calculated Electronic Properties of Metals*, Pergamon Press, NY (1978); https://doi.org/10.1016/B978-0-08-022705-4.50002-8.

[10] B.I. Shklovskii and A.L. Efros, *Electronic properties of doped semiconductors*, Springer-Verlag, Berlin, Heidelberg (1984); https://doi.org/10.1007/978-3-662-02403-4.

Л. Ромака[1], Ю. Стадник[1], В.А. Ромака[2], А. Горинь[1], В.В. Ромака[3,4], П. Демченко[1], П. Гаранюк[2]

Дослідження нового термоелектричного матеріалу, отриманого легуванням n-HfNiSn атомами Nb

[1]Львівський національний університет ім. І. Франка, Львів, Україна, lyubov.romaka@gmail.com;
[2]Національний університет “Львівська політехніка”, Львів, Україна, volodymyr.romaka@gmail.com;
[3]Технічний Університет м. Дрезден, кафедра неорганічної хімії II, Дрезден, Німеччина
[4]Інститут дослідження твердого тіла ім. Лейбніца, Дрезден, Німеччина vitaliy.romaka@tu-dresden.de

Досліджено структурні, кінетичні, енергетичні та магнітні властивості нового термоелектричного матеріалу $Hf_{1-x}Nb_xNiSn$, отриманого легуванням напівпровідника *n*-HfNiSn атомами Nb, уведеними у структуру шляхом заміщення у кристалографічній позиції 4*a* атомів Hf. Встановлено, що за концентрацій $x=0.02$ включно існує твердий розчин заміщення $Hf_{1-x}Nb_xNiSn$ атомів Hf ($5d^26s^2$) на атоми Nb ($4d^45s^1$). При цьому у структурі $Hf_{1-x}Nb_xNiSn$ генеруються дефекти донорної природи (Nb містить більше *d*-електронів, ніж атом Hf), а в забороненій зоні ε_g з’являються домішкові донорні стани ε_D. За концентрацій $0.02<x\leq0.05$, ймовірно, заміщення відбувається шляхом витіснення атомами Nb атомів Ni з позиції 4*a*, яку у вихідній сполуці HfNiSn займала статистична суміш атомів Hf та Ni. При цьому у структурі $Hf_{1-x}Nb_xNiSn$ генеруються дефекти акцепторної природи (Nb містить менше *d*-електронів, ніж атом Ni), а в забороненій зоні ε_g з’являються домішкові акцепторні стани ε_A. Співвідношення донорних та акцепторних станів визначає тип провідності $Hf_{1-x}Nb_xNiSn$. Показано, що напівпровідниковий твердий розчин $Hf_{1-x}Nb_xNiSn$ володіє високою ефективністю перетворення теплової енергії в електричну.

Ключові слова: напівпровідник, електропровідність, коефіцієнт термо-ерс, рівень Фермі.